Distinct transcriptomic reprogramming in the wheat stripe rust fungus during the initial infection of wheat and barberry

Jing Zhao[1, 2*], Wanlu Duan[1], Yiwen Xu[1], Ce Zhang[1], Long Wang[1], Jierong Wang[1], Song Tian[1], Guoliang Pei[2], Gangming Zhan[1, 2], Hua Zhuang[1, 2], Jie Zhao[1, 2], and Zhensheng Kang[1, 2*]

[1] College of Plant Protection, Northwest A&F University, Yangling, Shaanxi, People's Republic of China

[2] State Key Laboratory of Crop Stress Biology for Arid Areas, Northwest A&F University, Yangling, Shaanxi, People's Republic of China

*** Corresponding authors:**

Jing Zhao, email: zhaojing@nwsuaf.edu.cn;

Zhensheng Kang, email: kangzs@nwsuaf.edu.cn

Keywords:

wheat stripe rust; barberry; transcriptome; urediniospore; basidiospore; host specificity

Funding:

National Key Research and Development Program of China (no. 2018YFD0200402);

Research Funds for the Central Universities of China (no. 2452017405);

National Transgenic Key Project of China (no. 2016ZX08002-01);

Natural Science Basic Research Plan in Shaanxi Province of China (no. 2019JCW-18)

Abstract

Puccinia striiformis f. sp. *tritici* (*Pst*) is the causal agent of wheat stripe rust that causes severe yield losses all over the world. As a macrocyclic heteroecious rust fungus, it is able to infect two unrelated host plants: wheat and barberry. Its urediniospores infect wheat and cause disease epidemic, while its basidiospores parasitize barberry to fulfill the sexual reproduction. This complex life cycle poses interesting questions on the different mechanisms of pathogenesis underlying the infection of the two different hosts. In the present study, transcriptomes of *Pst* during the initial infection of wheat and barberry leaves were qualitatively and quantitatively compared. As a result, 142 wheat-specific expressed genes (WEGs) were identified, which was far less than 2,677 barberry-specifically expressed genes (BEGs). A larger proportion of evolutionary conserved genes were observed in BEGs than that in WEGs, implying a longer history of the interaction between *Pst* and barberry. Additionally, *Pst* differentially expressed genes (DEGs) between wheat at 1 dpi/2 dpi and barberry at 3 dpi/ 4dpi were identified by quantitative analysis. Gene Ontology analysis of these DEGs and expression patterns of *Pst* pathogenic genes, including those encoding candidate secreted effectors, cell wall degrading enzymes, and nutrient transporters, demonstrated that urediniospores and basidiospores exploited distinct strategies to overcome host defense systems. These results represent the first analysis of the *Pst* transcriptome in barberry and contribute to a better understanding of the evolutionary processes and strategies of different types of rust spores during the infection process on different hosts.

Rust fungi (*Pucciniales*) are the largest group of plant pathogenic fungi, with more than 8,000 described species (Aime et al. 2017). *Puccinia striiformis* f. sp. *tritici* (*Pst*), the causal agent of wheat stripe rust, is among the most important pathogens on wheat, and can cause severe yield losses. As a macrocyclic heteroecious rust fungus, *Pst* has five morphologically and functionally different spore forms and requires two specific but unrelated host plants to complete its life cycle (Zhao et al. 2016). In spring, teliospores overwintering on wheat debris germinate and produce basidiospores. Basidiospores infect barberry and form receptive hyphae and pycniospores on the upper surface of the barberry leaves. Upon fertilization of receptive hyphae by pycniospores, a dicaryotic mycelium develops that ultimately forms aeciospores on the lower surface of the barberry leaves. Aeciospores then infect wheat and produce asexual urediniospores that can infect wheat in repeated cycles and cause disease epidemics. At the late growing season of wheat, teliospores are produced, which allow *Pst* to survive the unfavorable summer and winter seasons.

This survival strategy of *Pst* poses interesting questions regarding the mechanisms of pathogenesis as well as nutrient uptake underlying the infection of two botanically unrelated host plants. Although having the same genetic background, urediniospores and basidiospores specifically infect wheat and barberry, respectively. In addition, different mechanisms are applied to penetrate host tissues: urediniospores infect wheat through stomata while basidiospores infect barberry through direct penetration of epidermal cells by appressorium (Jiao et al. 2017). It was therefore suggested that transcriptomic re-programming in these two types of spores might account for the *Pst* capacity of infecting two different hosts, especially at the initial stage of infection. In recent years, the transcriptomic profiling of cereal rust fungi and wheat interactions have been extensively studied (Chen et al. 2013; Dobon et al. 2016; Garnica et al. 2013;

Rutter et al. 2017; Yadav et al. 2016). Although mainly converging on the host aspect, these studies provide valuable information for deciphering rust pathogenicity and wheat immune response. However, transcriptomic studies on interactions between cereal rust fungi and their alternate hosts are less mentioned at present.

In order to successfully colonize wheat, *Pst* utilizes a set of pathogenicity-related genes and mechanisms to defeat the plant immune system and acquire nutrients to enable further growth and propagation. Previous studies have identified a lot of *Pst* candidate secreted effector protein (CSEP) genes by haustoria isolation and sequencing (Cantu et al. 2013; Upadhyaya et al. 2015). Recently, a number of *Pst* effectors playing critical roles during the infection of wheat have been identified and functionally characterized (Cheng et al. 2015; Cheng et al. 2017; Liu et al. 2016; Qi et al. 2019a; Wang et al. 2017; Xu et al. 2019; Yang et al. 2020; Zhao et al. 2018). For example, GSRE1 is a glycine-serine-rich effector which can suppress host immunity through targeting and blocking the nuclear localization of wheat transcription factor TaLOL2, a positive regulator of wheat reactive oxygen species (ROS) production (Qi et al. 2019a). Another important *Pst* effector is Pst_12806, which facilitate rust infection by interfering the function of chloroplasts, such as electron transport, photosynthesis, and chloroplast-derived ROS production (Xu et al. 2019). Recent studies have shown that the sexual cycle of *Pst* on barberry is responsible for the observed frequent virulence variations and the generation of new races of the pathogen (Zhao et al. 2016). However, very little is known about the specific mechanisms of *Pst* to infect its alternate host barberry.

In the present study, we analyzed and compared the global transcript profiles of *Pst* during infection of two different hosts. Sets of genes that are specifically expressed in either wheat or barberry were identified. Expression levels of *Pst* effector genes and

other genes involved in pathogenicity (such as plant cell wall degrading genes and nutrient transporter genes) in the initial stage of wheat and barberry infection were quantified and analyzed. Our data represents the first report of the transcriptome of *Pst* during the infection of barberry. This work provides a model to understand the evolutionary processes and strategies of different types of rust spores during the infection process on different hosts.

RESULTS

Histological analyses of *Pst* infection of barberry and wheat

Pst basidiospores and urediniospores use different ways to infect the respective hosts. Urediniospores geminate on wheat leaves and enter the plant tissue through stomata. By contrast, germinated basidiospores penetrate barberry leaf tissue directly through the epidermis (Jiao et al. 2017). To identify an appropriate time point for a comparison of the two types of infection, we compared the infection processes of basidiospores and urediniospores of *Pst* isolate CYR32 by histological observation (Fig. 1A). In wheat leaves inoculated by urediniospores, the formation of haustoria can be observed at 1 day post inoculation (dpi) followed by the formation of the secondary hyphae at 2 dpi. The penetration frequency for urediniospores raised from 17.0% at 1 dpi to 24.3% at 2 dpi, then remained around 26% at 3, 4, and 5 dpi (Fig. 1B). The infection process emanating from basidiospores on barberry seems to be more slowly. The ovate intra-epidermal vesicles (OIV) were not observed until 3 dpi and the secondary hyphae formed at 4 dpi (Fig. 1A). The penetration frequency for basidiospores raised from 11.1% at 3 dpi to 16.6% at 4 dpi and was held at 17.3% at 5 dpi (Fig. 1B). Therefore, wheat leaves at 2 dpi and barberry leaves at 4 dpi were selected for qualitative comparison. These two time points represent early stages of infection by urediniospores and basidiospores when parasitic relationship between *Pst* and the host plant has just been established.

Transcriptomes of *Pst* during infection of wheat and barberry

To clarify the different mechanisms deployed by urediniospores and basidiospores during the infection process of wheat and barberry, transcriptomes of both interactions were compared. Two *Pst* isolates, CYR32 and V26, were inoculated on wheat and barberry leaves. Then wheat leaf samples at 2 dpi and barberry leaf samples at 4 dpi

were collected. Since the fungal RNA at the early stage of infection represents only a small fraction of the total RNA from infected leaves, we constructed normalized cDNA libraries to increase the proportion of pathogen RNA that enabled us to detect expressed fungal genes more readily. Data from the normalized library were used for qualitative comparison of expressed genes of two *Pst* isolates in wheat and barberry. Meanwhile, barberry leaf samples from 3 and 4 dpi as well as wheat leaf samples from 1 and 2 dpi were collected, and non-normalized libraries were constructed for quantitative analysis of transcriptional levels for *Pst* genes during the early stage of infection of two hosts. Following quality filtering and data trimming, an average of 44.6 and 65 million high-quality reads per sample were produced for normalized and non-normalized samples, respectively (Table 1 and Supplementary Table S1). All of these reads were mapped onto PST-CY32 reference genome (Zheng et al. 2013). Since some reads that mapped to the reference genome did not align to predicted exons, we used our transcriptome data to generate an updated set of annotations using the software Cufflinks and the reference annotation based transcript (RABT) assembly pipeline (Roberts et al. 2011; Trapnell et al. 2012), which led to the annotation of another 2,712 genes (Supplementary Table S2) in addition to the 26,832 genes predicted from the reference genome. With the increasing of sequencing depth, each sample reached a plateau in the saturation curves independently of the isolates, host or time points (Supplementary Fig. S1), indicating a sufficient sequencing depth to cover a full transcriptome for all the samples.

For normalized samples, the percentage of reads aligned to the *Pst* genome were 14.47% (CYR32) and 19.79% (V26) for wheat leaves, and 13.05% (CYR32) and 9.80% (V26) for barberry leaves (Table 1). Among the 29,544 genes, transcripts of 18,328 genes (62.0%) were detected (with at least one read assigned). For isolate CYR32,

17,180 and 11,281 genes were found to be expressed in barberry and wheat, respectively. Similarly, for isolate V26, 14,032 and 10,550 *Pst* genes were found to be expressed in barberry and wheat, respectively (Fig. 2A; Supplementary Table S3). These results demonstrated that much more *Pst* genes were expressed during the infection of barberry than that of wheat. In addition, 8,277 genes were detected in all samples, indicating their essential roles in *Pst* infection of both hosts.

Compared to normalized samples, the percentages of reads mapped to *Pst* genome for non-normalized samples were apparently much lower (ranged from 0.55% to 1.25%), and few genes were detected as well (Supplementary Table S1). Similarly, there were still more gene transcripts detected in barberry than that in wheat, which was consistent with the results from the normalized samples.

Host-specifically expressed genes of *Pst* during the onset of pathogenesis in wheat or barberry

Expression levels from the normalized samples were used to characterize host-specifically expressed genes that are exclusively expressed in wheat or barberry at the early stage of infection. To this end, a threshold of Transcript per million (TPM) value above 2.0 in one host while below 2.0 in another host, and their ratio above 5.0 was defined for qualitative identification. Then, the analysis was performed for CYR32 and V26 separately and the intersection for two isolates were obtained. Finally, 142 wheat-specifically expressed genes (WEGs) were identified, which is far less than the 2,677 barberry-specifically expressed genes (BEGs) and 1,646 wheat-barberry-commonly expressed genes (WBEGs) identified (Supplementary Table S3).

Effectors are known as key pathogenic components that facilitate infection by modulating plant immunity and reprogramming host cell metabolisms. Among the 953 CSEP genes, 26 wheat-specifically expressed effector genes (WEEs) were identified.

Meanwhile 321 BEGs and 29 WBEGs were identified as barberry-specifically expressed effector genes (BEEs) and wheat-barberry commonly expressed effector genes (WBEEs), respectively. Despite the small number of WEEs, they account for a relative bigger proportion of WEGs (18.3%) than BEEs and WBEEs, which account for 12.0% and 1.8% of WEGs and WBEGs. In contrast, a higher percentage of functionally annotated genes were found in WBEGs (28.7%) than that in BEGs (9.1%) or WEGs (4.2%) (Fig. 2B).

Genes specifically expressed in wheat are "younger" than those in barberry

As a high proportion of functional annotated genes in BEGs, we speculated that these genes were evolutionary conserved among *Basidiomycetes*. To test this hypothesis, we identified orthologs of host specifically expressed genes from nine Basidiomycetes: *Puccinia striiformis* f. sp. *tritici* PST-78, *Puccinia graminis* f. sp. *tritici*, *Puccinia triticina* 1-1 BBBD Race 1, *Uromyces vicia-fabae*, *Melamspora larici-populina*, *Cronartium quercuum* f. sp. *fusiforme*, *Naiadella fluitans* ATCC 64713 v1.0, *Mixia osmundae* IAM and *Ustilago maydis* strain 521. Orthologs to BEGs were identified in a frequency of 40.12% to 89.65%. While, much less orthologs for WEGs were identified. For example, only 21.13% WEGs have orthologs in *U. maydis*, which was about one-half of that of BEGs (Table 2). In conclusion, genes specifically expressed in barberry tended to be evolutionary conserved while there were bigger proportion of young genes specifically expressed in wheat.

Identification of *Pst* differentially expressed genes during the infection of wheat and barberry

Expression levels from the non-normalized samples were used to a quantitative comparison of expression patterns of *Pst* genes in wheat and barberry. In total, 1,968 differentially expressed genes (DEGs) of *Pst* during the infection of wheat at 1 dpi/2 dpi and barberry at 3 dpi/4 dpi were identified (Supplementary Table S4). Among them,

there were 1,410 DEGs for samples from barberry at 3 dpi vs samples from wheat at 1 dpi, and 1,001 DEGs for barberry at 4 dpi vs wheat at 2 dpi, respectively. In total, there were 1,234 genes abundant in barberry at 3 dpi or 4dpi, while as 734 genes were abundant in wheat at 1 dpi or 2 dpi. However, there were no significant differences of expression levels between 3 dpi and 4 dpi in barberry, as well as expression levels between 1 dpi and 2 dpi in wheat, suggesting a gradual and consistent course of infection.

Puccinia striiformis f. sp. *tritici* DEGs between hosts were categorized into functional classes using Gene Ontology (GO) to identify specific terms they were involved in (Supplementary Table S5). As shown in Fig. 4, DEGs abundant in barberry at 3 dpi or 4 dpi were enriched in hydrolase activity (acting on carbon-nitrogen bonds) (GO:0016810), FMN binding (GO:0010181), carbohydrate metabolic process (GO:0005975), oxidoreductase activity (GO:0016491), and calcium ion binding(GO:0005509). In contrast, DEGs abundant in wheat at 1 dpi or 2 dpi were overrepresented by hydrolase activity (hydrolyzing O-glycosyl compounds) (GO:0004553), carbohydrate metabolic process (GO:0005975), channel activity (GO:0015267), substituted mannan metabolic process (GO:0006080), mannan endo-1,4-beta-mannosidase activity (GO:0016985), and chromatin remodeling (GO:0006338).

The analysis of KEGG pathway was also performed to identify metabolic pathways involving *Pst* DEGs (Supplementary Table S6; Fig. S4). As a result, DEGs abundant in barberry were mainly enriched in Starch and sucrose metabolism (ko00500), Melanogenesis (ko04916), cAMP signaling pathway (ko04024), Aldosterone synthesis and secretion (ko04925), and Kaposi sarcoma-associated herpesvirus infection (ko05167); and DEGs abundant in wheat were mainly enriched in MAPK signaling pathway (ko04011), transcription factors (BR:ko03000), protein phosphatases and

associated proteins (BR:ko01009), and pentose and glucuronate interconversions (ko00040).

Expression profile of CSEP repertoires in wheat and barberry and six BEEs suppress BAX-induced cell death in tobacco

The expression patterns of 230 differentially expressed CSEP genes were clustered (Fig. 5; Supplementary Table S4). Apparently, most of CSEP genes abundant in wheat fall into the clade I representing genes with higher expression levels in wheat at 1 or 2 dpi than that inbarberry at 3 or 4 dpi . Unsurprisingly, nearly all WEEs (24 out of 26) were identified as differentially expressed CSEP genes and attributed to clade I, and there were 7 differentially expressed CSEP genes abundant in wheat belonged to WBEEs because of their absolute higher expression in both hosts. Similarly, clade II contains all the 174 differentially expressed CSEP genes abundant in barberry, in which 151 genes belonged to 321 BEEs.

One of the most important function of pathogen effectors is to suppress the host immune response, such as the hypersensitive cell death. A number of *Pst* effectors identified from *Pst*-wheat interaction have been proven to function in suppression of wheat cell death (Qi et al. 2019a; Xu et al. 2019). Since no obvious cell death of barberry leaves was observed during the *Pst* infection, we speculated that those BEEs might play similar roles in barberry as in wheat. To validate their role in the suppression of cell death, 60 BEEs were transiently expressed in tobacco together with BAX, which has been shown to be an inducer of plant cell death. Finally, six BEEs were proven to inhibit BAX-induced cell death in tobacco (Fig. 6), suggesting their critical role in impairing the plant immune system.

Expression patterns of host cell wall degrading genes between wheat and barberry

Plant cuticle and cell wall are the first barriers to block the infection of *Pst*. To achieve successful penetration, *Pst* releases a set of cell wall and cuticle degrading enzymes, such as pectinase, cellulase, hemicellulase and cutinase. The genes encoding these enzymes were identified and their expression levels were compared during the infection of wheat and barberry (Fig. 7A). Seven genes encoding pectinases were identified and all of them were expressed in barberry, while they were nearly undetectable in wheat leaves. Among seven genes encoding cellulase, three had little or no expression in both hosts, and four were highly expressed in barberry and one was moderately expressed in wheat. For ten genes encode hemicellulases, all of them were expressed in barberry at moderate or low levels while none of them was detected in the wheat. Remarkably, among the eight genes encoding secreted cutinases, two were highly expressed in wheat and five were exclusively expressed in barberry. Since it was reported that the abundance of genes encoding cell wall degrading enzymes in fungal genome were related to the host cell wall compositions (O'Connell et al. 2012), we measured the contents of cellulose, hemicellulose, pectin and lignin of wheat and barberry leaves to test if they are connected with the expression levels of the corresponding degradation genes (Fig. 7B). The results revealed a higher content of pectin in barberry leaves, which may be the reason for the extremely high transcriptional level of *Pst* pectinase genes during the infection of barberry. However, although with higher expression levels of *Pst* cellulase and hemicellulase genes in the infected leaves of barberry, there was no significant difference in the content of cellulose and hemicellulose between the two hosts. In general, *Pst* uses different sets of CAZymes depending on the host.

Expression profiles of nutrient transporters in wheat and barberry

As an obligate biotrophic pathogen, *Pst* needs to uptake nutrients from living cells

of its host through different kinds of transporters located in the haustorial membrane (Voegele et al. 2011). To dissect the mechanisms by *Pst* nutrient acquisition from wheat and barberry, transcriptional profiles of genes involving hexose and amino acid transporters were analyzed. Among the 35 hexose transporter genes identified in *Pst*, most of them were expressed in both wheat and barberry (with a threshold of average TPM value ≥ 2.0 for at least one time point) and exhibited no apparent difference in expression levels between the two hosts (Supplementary Fig. S3). However, three hexose transporter genes, *PSTCY32_06236*, *PSTCY32_07224* and *PSTCY32_13723*, were preferentially expressed in wheat and one hexose transporter encoding gene *PSTCY32_05623* was preferentially expressed in barberry (Supplementary Fig. S3). For the 25 amino acid transporter genes identified in *Pst* genome, two ACT family members genes, *PSTCY32_06701* and *PSTCY32_00575* were found to be differentially expressed and abundant in barberry (Supplementary Fig. S4). However, an amino acid transporter encoding gene from LAT family, *PSTCY32_26693*, exhibited higher expression levels during the infection of wheat than that of barberry (Supplementary Fig. S4).

DISCUSSION

The in-depth transcriptomic profiling of *Pst* presented in this study allows a comprehensive understanding of common and diverse mechanisms of *Pst* pathogenesis on its two hosts. By constructing normalized cDNA libraries of *Pst* infected wheat and barberry leaves, we obtained sufficient sequencing depth (43.0x to 62.7x) to compare these transcriptomes of *Pst* during early stages of infection. The proportion of reads mapped to the *Pst* reference genome ranged from 9.80% to 19.79%. This is much higher than that in similar studies (Dobon et al. 2016). On this basis, genes expressed in wheat and/or barberry during *Pst* infection were identified by qualitative analysis. Overall, 18,328 genes were expressed in at least one sample, and more genes were detected in barberry than in wheat, suggesting that more genes or gene products are involved in barberry infection and a more complex interaction between *Pst* and its aecial host barberry. This finding could at least partially be explained by the fact that *Pst* sexual reproduction on barberry was more complicated than asexual multiplication on wheat.

The interactions of asexual urediniospores and telial host have been extensively studied (Dobon et al. 2016; Garnica et al. 2013; Schwessinger et al. 2018). However, little was known about the transcriptome of rust fungi at sexual stage. Only a few transcriptomic studies have focused on basidiospores during the infection of its aecial host. Although at a limited scale, the transcriptome across all life cycle stages of *Puccinia triticina* was estimated and expression profiles of CSEPs in its two hosts wheat and meadow rue (*Thalictrum speciosissimum*) were assessed (Cuomo et al. 2017). In another study, transcriptomes of *Cronartium ribicola* aeciospores, urediniospores and two infection stages on the aecial host (western white pine) were compared, while no infection stage on the telial host (*Ribes nigrum*) was included (Liu et al. 2015). For *M. larici-populina* (*Mlp*), the causal agent of poplar rust, transcriptomic data for basidia,

infected larch needles, urediniospores, and infected poplar leaves were compared (Lorrain et al. 2018). Overall, 1,436 and 1,531 genes were found to be specifically expressed at the sexual and the asexual stage, respectively. In the present study, time points representing haustoria and secondary hyphal formation (4 dpi of basidiospores on barberry and 2 dpi of urediniospores on wheat) were chosen to represent the early stage of *Pst* infection. The time point choice of the sampling provided comparable parallel datasets and allowed us to determine gene expression more precisely and identify host-specific expressed genes of significance for infection. Although a set of *Pst* genes have been found to be host-specific, more genes were simultaneously detected during the two different host colonization, despite that these two plants being phylogenetically distant. This finding was consistent with the transcriptomic study on the infection of poplar and larch by *Mlp* (Lorrain et al. 2018).

Effectors are key players for pathogenicity. The significant overrepresented CSEPs in WEGs or BEGs (18.3% and 12.0% vs overall CSEP proportion of 3.2%) were observed. Similarly, a relative high proportion of small secreted proteins (SSP) was found to be enriched in highly expressed genes specific to poplar or larch. These results suggested that CSEPs may also contribute to the host specificity. Actually, a large number of research results have proven the roles of pathogen CSEPs in host specificity (Borah et al. 2018). For example, a recent study demonstrated that several effector proteins recognized by corresponding resistance genes in barley or related grass determine the host range of powdery mildew pathogen (Bourras et al. 2019).

In this study, a quantitative analysis was performed to allow us to compare the transcriptional levels of different sets of pathogenic genes during the infection of two hosts. In general, the transcription patterns in different hosts were consistent with the data obtained in qualitative analysis using normalized library. Additionally, no obvious difference was observed between the *Pst* transcriptome at 1 dpi and 2 dpi in wheat, as

well as between 3 dpi and 4 dpi in barberry. However, there are still some genes exhibited clear transition in expression during the early infection, such as three WEEs (PSTCY32_00469, PSTCY32_18558, and PSTCY32_20164) which have sharp increased expression levels from 1 to 2 dpi. These effector genes may have critical roles during the initial penetration of wheat by *Pst*.

To successfully penetrate into plant tissue and cell, a rust fungus needs to secrete different sets of enzymes (glycohydrolase) to degrade plant cuticle and cell wall. During the *Pst* infection of barberry, most of the pectinase genes, as well as cellulose and hemicellulose genes, expressed with high levels while no or very low levels were detected during the infection of wheat. This might be due to the higher content of pectin in barberry cell wall, but a more possible explanation would be the extra-thick outer wall of epidemic cells compared to the mesophyll cells (Amanda et al. 2016). In addition, it was unexpected that two cutinases were highly expressed in wheat while *Pst* penetrated into wheat leave tissue through stomata. A reasonable explanation should be that the wheat cuticle destroyed by cutinases may facilitate the adhesion of the urediniospores germ tubes on the leaf surface, as what had been found in broad bean rust (Deising et al. 1992; Schafer, 1993). The adhesion of germlings on epidermis of wheat leaves are of extra significance since no appressoria were formed during the *Pst* infection of wheat (Moldenhauer et al. 2006). Thus, *Pst* uses different sets of CAZymes not only depending on host cell-wall composition, but also related to the host-tissue penetration mechanisms of basidiospores and urediniospores. Conversely, more common genes involved nutrient absorption were expressed both in wheat and in barberry, indicating that *Pst* uses a similar way to absorb nutrients from wheat and barberry.

A heteroecious grass rust requires two phylogenetically different hosts to complete

their life cycle. Usually, they undergo sexual reproduction on one plant species and asexual propagation on another unrelated plant species. However, it has long been unclear that the biological significance of this life style and the relationship of the two hosts. By the combination of phylogenetic and hologenetic analysis, Leppik et al. (1959) postulated that the aecial host of a cereal rust fungus, *Berberidaceae* and *Rhamnaceae* or other arboreous families of primitive angiosperms, might be the primary host, and graminaceous plants are the secondary host of a heteroecious grass rust fungus. Whether the telia or the aecial stage is more primitive and ancestral for a grass rust fungus remains considerably controversial due to the lack of experimental evidence. In our study, over 300 effectors were specifically expressed in barberry, and a higher proportion of conserved genes were preferentially expressed in barberry than that in wheat. These results implied a long co-evolutionary relationship between *Pst* and barberry. As a matter of fact, *Berberidaceae* plants, belonging to primitive angiosperms and originating from 146-113 million years ago, are evolutionarily older than grasses (Poaceae originates from 65-110 million years ago) (https://www.mobot.org/MOBOT/research/APweb/), which makes them interact with rust fungi earlier according to the coevolutionary relationship between a rust fungus and its host (Aime et al. 2018). Furthermore, besides of *P. striiformis*, *Berberis* spp. are aecial hosts of a wide range of grass rust fungi, including at least seven *Puccinia* spp. (e.g. *P. graminis*, *P. striiformis*, *P. montanensis*, *P. brachypodii*, *P. pigmea*, *P. koeleriae*, and *P. arrhenatheri*) (Bartaula et al. 2019, Huang et al. 2019). If barberry as the primary host for *Pst* is accepted, it will raise a question that how the ancestor of barberry rust fungi completed their life cycle since the aeciospores produced on barberry could not come back (Jiao et al. 2017). One possibility would be that the ancestor of a barberry rust fungus had a more ancient telial host than *Berberidaceae*,

such as *Cupressacea*. Another possibility is that the ancient rust fungus spent all their lives on barberry like *Cumminsiella mirabilissima*, which produces all five types of spores on mahonia, a kind of *Berberidaceae* plant that is closely related to barberry and can serve as the aecial host of *Pst* (Ruske and Dörfelt 2010; Wang and Chen, 2013). Several studies have reported that uredia and telia of *P. graminis* f. sp. *tritici* can be produced on barberry under natural and laboratory conditions (Critopoulos 1947; Newton and Johnson 1937). Thus, the ancestor of barberry rust fungi may have adapted themselves to the emerging grasses in the neighborhood and switched the telial stage to them. Altogether, the analysis of orthologous genes for host-specific expressed genes in this study offers a new perspective for origin and evolution study of rust fungi.

So far, numerous *Pst* effectors have been identified and their pathogenic roles in pathogen-wheat interaction have been extensively revealed (Cheng et al. 2015; Cheng et al. 2017; Qi et al. 2019a; Xu et al. 2019; Yang et al. 2020; Zhao et al. 2018). With the knowledge of preferential or specific expression in wheat or barberry, we identified 6 BEEs that were capable of suppression BAX-induced cell death in tobacco. Future functional characterization of these genes may help to develop resistance barberry materials by host-induced gene silencing strategies (Qi et al. 2019b). In addition, those candidate effectors expressed in both hosts may represent “core effectors” that conserved among rust fungi and play key roles in the rust basic pathogenicity. More attentions should be paid to the in-depth study of these “core effectors” to discover the molecular basis for rust pathogenicity.

Experimental Procedures

Plant materials and inoculation

Seedlings of the *Pst*-susceptible wheat cultivar MX169 were grown in the

greenhouse at 16℃ and 16:8 light:dark cycle. Ten-day old seedlings were inoculated with fresh urediniospores of *Pst* strain CYR32 and V26, and incubated for 24 h in 100% humidity at 9℃ in the dark. Barberry (*Berberis shensiana*) plants were grown in under 70% relative humidity at 16℃ and 16:8 light:dark cycle. Three to four month old barberry seedlings were inoculated with CYR32 and V26 basidiospores produced from germinating teliospores according to the method described by Zhao J. et al. (2013).

Histological treatment and observation

The wheat leaf segments and barberry leaf discs infected by *Pst* were fixed and decolorized in decolorizing solution (ethyl alcohol:acetic acid, 1:1 v/v) and followed by immersed overnight in chloral hydrate. The decolorized samples were then autoclaved in 1.5 ml of 1M KOH at 121°C for 5-6 min. Those samples were washed three times with 50 mM Tris-HCl (pH 7.4) for 15 min and stained with 20 μg/ml wheat germ agglutinin (WGA) conjugated to Alexa-488 solution (cat. no. W11261, Thermo Fisher Scientific). The fluorescent stained samples were observed under blue-light excitation (excitation wavelength 450–480 nm, emission wavelength 515 nm) using an Olympus BX-53 microscope (ocular: 10×; objective: 20×) and CellSens Entry software (version: V1.7). Penetration frequencies for *Pst* urediniospores on wheat leaves represent the percentage of germinated spores penetrating the mesophyll cells and forming haustoria. Penetration frequencies for *Pst* basidiospores on barberry leaves represent the percentage of germinated spores penetrating into epidermal cells and forming ovate intra-epidermal vesicle.

RNA extraction, library preparation, and sequencing

Entire leaf tissue was taken from barberry plants at 3 and 4 days after inoculation and wheat plants at 1 and 2 days post inoculation, and then immediately frozen in liquid nitrogen. Frozen leaf samples were then ground in liquid nitrogen, and total RNA was isolated using the QIAGEN (Doncaster, Australia) Plant RNeasy kit following the manufacturer's instructions. RNA was checked for integrity on an Agilent 2100 Bioanalyzer. First strand cDNA was synthesized using random hexamer primer and M-MuLV Reverse Transcriptase. Normalized and non-normalized cDNA libraries were generated for qualitative and quantitative analyses of *Pst* transcriptome. For qualitative analysis, normalized cDNA libraries was constructed using the DSN (Duplex-specific nuclease)-normalization technology with a high gene discovery rate (Bogdanova et al. 2008). Briefly, after denaturation of double-stranded (ds) cDNA flanked with adapters, it was subjected to renature at 68°C, and treated with DSN (evrogen Russia). During renaturation, abundant transcripts are converted to the double-stranded form more effectively than those that are less frequent. Thus, two fractions are formed, specifically, a ds-fraction of abundant cDNA and a normalized single-stranded (ss) cDNA. The ds cDNA fraction is then degraded by DSN. After that, the undigested fragments were then amplified by long distance polymerase chain reaction (PCR). The products were then random fragmented and adapters for Illumina sequencing were ligated. Finally, the resulting tagged cDNA libraries were used for 150-bp paired-ends sequencing on the Illumina Hi-Seq 2000 Platform (Illumina, San Diego, CA, USA). For quantitative

analysis, non-normalized cDNA libraries were constructed following the manufacturers' instructions of RNA transcriptome discovery Kit (K02421-TS, Gnomegen). Amplified cDNA fragments were then used for 150-bp paired-ends sequencing on the Illumina Hi-Seq 2000 Platform.

Gene expression analysis and orthologous gene identification

Raw reads were processed to trim adapter sequences and remove low-quality sequences with Q20 filtering using Trimmomatic v0.32 (Bolger et al. 2014) with default settings, and then evaluated by Fastqc v0.10.0 (Andrews et al. 2010). After adapter trimming and quality trimming, the clean reads were mapped to the updated reference genome of *Pst* strain CYR32 (Zheng et al. 2013) using tophat2 (v2.1.0) with Bowtie2 (Kim et al. 2013). Novel transcripts were identified using Cufflinks (version 2.2.1) in "reference annotation based transcript assembly" mode with sequence bias correction enabled. Then, the transcript abundances (inferred in transcript per million, TPM) were calculated by Samtools (Li et al. 2009).

Expression levels from normalized samples were used to characterize host-specific expressed genes. *Pst* gene with a TPM values above 2.0 in wheat and below 2.0 in barbery, and the ratio between two host above 5.0 for both *Pst* isolates were defined as wheat-specific expressed genes (WEGs). Likewise, gene with a TPM values above 2.0 in barley and below 2.0 in wheat, and the ratio between two hosts above 5.0 for both *Pst* isolates were defined as barberry-specifically expressed genes (BEGs). Genes with TPM values above 2.0 in both hosts were designated as WBEGs (wheat and barberry

expressed genes). For orthologous gene identification, the protein sequence of each host-specifically expressed gene was used as query to search against each other Basidiomycetes genome data using BLASTP with an E-value below 10^{-3}.

Differential expression analyses were performed for *Pst* genes with the edgeR R/Bioconductor package (Robinson et al. 2010). The read counts were first normalized using the TMM (trimmed mean of M-values) method of the edgeR and then the logarithm of the CPM (counts per million) to the base 2 were used for further statistical analysis using the Limma R/Bioconductor package. Differentially expressed genes (DEGs) were identified based on a fold change $\geqslant$2 and an FDR (false-discovery-rate) $\leqslant$0.05 between samples.

Identification of effector genes, cell wall degradation genes and transporter genes

Candidate secreted effector proteins were predicted using bioinformatics software according to their biological characteristics. Briefly, *Pst* secreted proteins carrying a signal peptide (SP) were identified by SignalP 4.0 (Petersen et al. 2011) with D-cutoff value of 0.34. Then transmembrane proteins (contains at least one transmembrane domain after the first 60 amino acids or at least two transmembrane domains in total) were predicted by TMHMM 2.0 (Krogh et al. 2001) and excluded from the *Pst* secretome. Finally CSEPs were predicted by EffectorP v2.0 (Sperschneider et al. 2018).

To identify cell wall degradation proteins, *Pst* protein sequences were subjected to dbCAN2 meta server to identify secreted CAZymes by HMMER program (http://bcb.unl.edu/dbCAN2/index.php) (Zhang et al. 2018). Proteins annotated as GH6,

GH7, GH12, GH45, GH61, GH74, and GH94 were attributed to the cellulase. Similarly, CE1, GH10, GH11, GH26, GH29, GH43, GH51, GH53, GH54, GH62, GH67, and GH93 belong to hemicellulase. CE8, PL1, PL2, PL3, PL4，PL9, PL10, GH28, GH78, and GH88 belong to pectinase. While proteins annotated as CE5 CAZymes belong to cutinase (Zhao Z. et al. 2013).

To identify *Pst* hexose transporters, the protein sequences of yeast (*Saccharomyces cerevisiae*) hexose transporters HXT1~HXT7 (Luyten et al. 2002) were used as queries to search against the CYR32 genome using the tBLASTn program. Finally, 35 *Pst* hexose transporter genes with *P*-value less than 10e-3 were identified. Likewise, using amino acid transporter proteins reported in a previous article as seed sequences (Struck 2015), we identified 25 amino acid transporter genes in the CYR32 genome.

Go and KEGG analysis of *Pst* DEGs during the infection of wheat and barberry

GO annotation was performed by searching 29,544 *Pst* protein sequence against four databases including pfam, PANTHER, CDD and COIL using Interproscan v5.39-77.0. KEGG annotation was performed by online tools KAAS (https://www.genome.jp/kaas-bin/kaas_main). Then the R package of clusterProfiler were used for enrichment analysis (Yu et al. 2012).

Quantitative determination of cell wall composition

Wheat and barberry leaf samples at 2-week stage and six-month stage respectively were collected and dried to a constant weight at 50°C. Then the dried leaf samples (0.1 g) were ground into fine powders, and the cell wall materials (CMW) were extracted

by removing the alcohol-soluble components and starch using ethanol/acetone extraction and α-Amylase digestion according to the methods described by Pettolino et al. (2012).

Total cellulose contents of the cell wall from wheat and barberry leaf samples were measured using the colorimetric Anthrone assay, according to the method as previously reported (Updegraff 1969; Foster et al. 2010b). Briefly, the obtained CWM was firstly hydrolyzed by 2 M trifluoroacetic acid (TFA). After centrifugation, the precipitate and supernatant were used for cellulose and hemicellulose analyzing, respectively. For cellulose measurement, the precipitate was incubated with 1 mL Updegraff reagent (Acetic acid: itric acid: water, 8:1:2 v/v) at 100°C for 1 h. and pretreated with 72% sulfuric acid for Saeman hydrolysis. For hemicellulose measurement, the supernatant was directly treated with 72% sulfuric acid. Then the released glucose was reacted with 0.2% Anthrone reagent at 100°C for 10 min, and the resulting blue reaction products were measured at 620 nm wave length. The contents of cellulose and hemicellulose were presented as equivalents of glucose used in the standard curve.

Total pectin were extracted from CWM with ammonium oxalate, and pectin contents were determined according to the colorimetric method at wave length of 520 nm as described by Blumenkrantz and Asboe-Hansen (1973). The contents of pectin were presented as equivalents of galacturonic acid used as the standard.

The lignin content of the leaf samples was determined using the acetyl bromide method as previously reported (Hatfield et al. 1999; Foster et al. 2010b). Lignin was

quantified with the acetyl bromide method using absorbance values at 280 nm. An extinction coefficient of 17.75 was used to calculate the lignin content of all samples.

All the absorbance measurement were performed by a Synergy H1 Hybrid Multi-Mode Microplate Reader (BioTek instrumnets, USA). Four biological replicates were performed for each experiment. T-tests were used to assess statistical significance.

Agrobacterium tumefaciens infiltration assays

To screen *Pst* candidate effectors that can suppress the Bax-induced cell death in *N. benthamiana*, we infiltrated *A. tumefaciens* cells containing pGR107-PVX constructs expressing candidate effector genes or GUS genes (as a control) into leaves followed 24 h later by inoculation at the same site with *A. tumefaciens* cells carrying pGR107-PVX-Bax. Symptoms were observed and recorded at 5 dpi. For protein extraction, *N. benthamiana* leaves were frozen in liquid nitrogen 2 days after agroinfiltration and ground to a fine powder with a mortar and pestle. Protein extraction and nuclear-cytoplasmic fractionation were performed as described by Wang et al. (2011).

Acknowledgement

We are grateful to the review of this manuscript by Prof. Ralf Thomas Vögele, Institute for Phytomedicine, University of Hohenheim, German.

Data Availability Statement

The data that support the findings of this study are openly available in NCBI Sequence Read Archive, reference number PRJNA637808.

Author Contributions

Jing Zhao, Jie Zhao and Zhensheng Kang conceived and designed the experiment. Long Wang, Song Tian and Hua Zhuang prepared the leaf samples for sequencing. Wanlu Duan and Yiwen Xu measured the concentration of cell wall components and screened the candidate effectors in tobacco. Ce Zhang performed the histological observations. Jing Zhao, Jierong Wang and Guoliang Pei analyzed the data. Jing Zhao and Zhensheng Kang wrote the paper. All the authors have seen and approved the manuscript in final version prior to submission.

References

Aime, M. C., Bell, C. D., and Wilson, A. W. 2018. Deconstructing the evolutionary complexity between rust fungi (*Pucciniales*) and their plant hosts. Stud. Mycol. 89:143–152.

Aime, M. C., McTaggart, A. R., Mondo, S. J., and Duplessis, S. 2017. Phylogenetics and phylogenomics of rust fungi. Pages 267–307 in: Fungal Phylogenetics and Phylogenomics. Academic Press, New York, U.S.A.

Amanda, D., Doblin, M. S., Galletti, R., Bacic, A., Ingram, G. C., and Johnson, K. L. 2016. DEFECTIVE KERNEL1 (DEK1) Regulates Cell Walls in the Leaf Epidermis. Plant Physiol. 172:2204-2218.

Andrews, S. 2010. FastQC: a quality control tool for high throughput sequence data. Available online at: http://www.bioinformatics.babraham.ac.uk/projects/fastqc

Bartaula, R., Melo, A. T. O., Kingan, S., Jin, Y., and Hale, I. 2019. Mapping non-host resistance to the stem rust pathogen in an interspecific barberry hybrid. BMC Plant Biology 19:319.

Blumenkrantz, N. and Asboe-Hansen, G. 1973. New method for quantitative determination of uronic acids. Anal. Biochem. 54:484-489.

Bogdanova, E. A., Shagin, D. A., and Lukyanov, S. A. 2008 Normalization of full-length enriched cDNA. Mol. Biosyst. 4**:**205–212.

Borah, N., Albarouki, E., and Schirawski, J. 2018. Comparative methods for molecular determination of host-specificity factors in plant-pathogenic fungi. Int. J. Mol.

Sci. **19**:863.

Bourras, S., Kunz, L., Xue, M. F., Praz, C. R., Muller, M. C., Kalin, C., Schlafli, M., Ackermann, P., Fluckiger, S., Parlange, F., Menardo, F., Schaefer, L. K., Ben-David, R., Roffler, S., Oberhaensli, S., Widrig, V., Lindner, S., Isaksson, J., Wicker, T., Yu, D. Z., and Keller, B. 2019. The AvrPm3-Pm3 effector-NLR interactions control both race-specific resistance and host-specificity of cereal mildews on wheat. Nature Communications, **10**:2292.

Cantu, D., Segovia, V., MacLean, D., Bayles, R., Chen, X. M., Kamoun, S., Dubcovsky, J., Saunders, D. G. O., and Uauy, C. 2013. Genome analyses of the wheat yellow (stripe) rust pathogen *Puccinia striiformis* f. sp *tritici* reveal polymorphic and haustorial expressed secreted proteins as candidate effectors. BMC Genomics 14:270.

Chen, C. J., Chen, H., Zhang, Y., Thomas, H. R., Frank, M. H., He, Y. H., and Xia, R. 2020. TBtools: An integrative toolkit developed for interactive analyses of big biological data. Mol. Plant 13:1194-1202.

Chen, X., Coram, T., Huang, X., Wang, M. and Dolezal, A. 2013. Understanding molecular mechanisms of durable and non-durable resistance to stripe rust in wheat using a transcriptomics approach. Curr. Genomics 14:111–126.

Cheng, Y. L., Wang, X. J., Yao, J. N., Voegele, R. T., Zhang, Y. R., Wang, W. M., Huang L. L., and Kang Z. S. 2015. Characterization of protein kinase PsSRPKL, a novel pathogenicity factor in the wheat stripe rust fungus. Environ. Microbiol.

17:2601–2617.

Cheng, Y. L., Wu, K., Yao, J. N., Li, S. M., Wang, X. J., Huang, L. L., and Kang Z. S. 2017. *PST*ha5a23, a candidate effector from the obligate biotrophic pathogen *Puccinia striiformis* f. sp *tritici*, is involved in plant defense suppression and rust pathogenicity. Environ. Microbiol. 19:1717–1729.

Critopoulos, P. D. 1947. Production of teliospores and uredospores of *Puccinia Graminis* on *Berberis Cretica* in nature. Mycologia 39:145–151.

Cuomo, C. A., Bakkeren, G., Khalil, H. B., Panwar, V., Joly, D., Linning, R., Sakthikumar, S., Song, X., Adiconis, X., Fan, L., Goldberg, J. M., Levin, J. Z., Young, S., Zeng, Q. D., Anikster, Y., Bruce, M., Wang, M. N., Yin, C. T., McCallum, B., Szabo, L. J., Hulbert, S., Chen, X. M., and Fellers, J. P. 2017. Comparative analysis highlights variable genome content of wheat rusts and divergence of the mating loci. G3-Genes Genom. Genet. 7:361-376.

Deising, H., Nicholson, R. L., Haug, M., Howard, R. J. and Mendgen, K. 1992. Adhesion pad formation and the involvement of cutinase and esterases in the attachment of uredospores to the host cuticle. Plant Cell 4:1101–1111.

Dobon, A., Bunting, D. C. E., Cabrera-Quio, L. E., Uauy, C., and Saunders, D. G. O. 2016. The host-pathogen interaction between wheat and yellow rust induces temporally coordinated waves of gene expression. BMC Genomics 17:380.

Foster, C. E., Martin, T. M., and Pauly M. 2010a. Comprehensive compositional analysis of plant cell Walls (Lignocellulosic biomass) Part I: Lignin. JoVE-J.

Vis. Exp. 37:1745.

Foster, C. E., Martin, T. M., and Pauly M. 2010b. Comprehensive compositional analysis of plant cell Walls (Lignocellulosic biomass) Part II: Carbohydrates. JoVE-J. Vis. Exp. 37:1837.

Garnica, D. P., Upadhyaya, N. M., Dodds, P. N., and Rathjen, J. P. 2013. Strategies for wheat stripe rust pathogenicity identified by transcriptome sequencing. Plos One 8:e67150.

Hatfield, R. D., Grabber, J., Ralph, J., and Brei, K. 1999. Using the acetyl bromide assay to determine lignin concentrations in herbaceous plants: Some cautionary notes. J. Agr. Food Chem. 47:628-632.

Huang, S., Zuo, S., Zheng, D., Liu, Y., Du, Z., Kang, Z., and Zhao, J. 2019. Three formae speciales of *Puccinia striiformis* were identified as heteroecious rusts based on completion of sexual cycle on *Berberis* spp. under artificial inoculation Phytopathol. Res. 1:14.

Jiao, M., Tan, C. L., Wang, L., Guo, J., Zhang, H. C., Kang, Z. S., and Guo, J. 2017. Basidiospores of *Puccinia striiformis* f. sp *tritici* succeed to infect barberry, while Urediniospores are blocked by non-host resistance. Protoplasma 254:2237–2246.

Jones, P., Binns, D., Chang, H. Y., Fraser, M., Li, W. Z., McAnulla, C., McWilliam, H., Maslen, J., Mitchell, A., Nuka, G., Pesseat, S., Quinn, A. F., Sangrador-Vegas, A., Scheremetjew, M., Yong, S. Y., Lopez, R., and Hunter, S. 2014.

InterProScan 5: genome-scale protein function classification. Bioinformatics 30:1236-1240.

Kim, D., Pertea, G., Trapnell, C., Pimentel, H., Kelley, R., and Salzberg, S. L. 2013. TopHat2: accurate alignment of transcriptomes in the presence of insertions, deletions and gene fusions. Genome Biology 14:R36

Krogh, A., Larsson, B., von Heijne, G., and Sonnhammer, E. L. L. 2001. Predicting transmembrane protein topology with a hidden Markov model: Application to complete genomes. J. Mol. Biol. 305:567–580.

Leppik, E. E. 1959. Some viewpoints on the phylogeny of rust fungi. III. Origin of grass rusts. Mycologia 51:512–528.

Li, H., Handsaker, B., Wysoker, A., Fennell, T., Ruan, J., Homer, N., Marth, G., Abecasis, G., Durbin, R., and Proc, G. P. D. 2009. The sequence Alignment/Map format and SAMtools. Bioinformatics 25:2078-2079.

Liu, J., Guan, T., Zheng, P. J., Chen, L. Y., Yang, Y., Huai, B. Y., Li, D., Chang, Q., Huang, L. L., and Kang, Z. S. 2016. An extracellular Zn-only superoxide dismutase from *Puccinia striiformis* confers enhanced resistance to host-derived oxidative stress. Environ. Microbiol. 18:4118–4135.

Liu, J. J., Sturrock, R. N., Sniezko, R. A., Williams, H., Benton, R., and Zamany, A. 2015. Transcriptome analysis of the white pine blister rust pathogen *Cronartium ribicola*: de novo assembly, expression profiling, and identification of candidate effectors. BMC Genomics 16:678.

Lorrain, C., Marchal, C., Hacquard, S., Delaruelle, C., Petrowski, J., Petre, B., Hecker, A., Frey, P., and Duplessis, S. 2018. The rust fungus *Melampsora larici-populina* expresses a conserved genetic program and distinct sets of secreted protein genes during infection of its two host plants, larch and poplar. Mol. Plant-Microbe Interact. 31:695–706.

Luyten, K., Riou, C., and Blondin, B. 2002. The hexose transporters of *Saccharomyces cerevisiae* play different roles during enological fermentation. Yeast 19:713–726.

Moldenhauer, J., Moerschbacher, B. M., and Van der Westhuizen, A. J. 2006. Histological investigation of stripe rust (*Puccinia striiformis* f. sp *tritici*) development in resistant and susceptible wheat cultivars. Plant Pathol. 55:469–474.

Newton, M. and Johnson, T. 1937. Production of uredia and yelia of *Puccinia graminis* on *Berberis vulgaris*. Nature 139:800–801.

O'Connell, R. J., Thon, M. R., Hacquard, S., Amyotte, S. G., Kleemann, J., Torres, M. F., Damm, U., Buiate, E. A., E*Pst*ein, L., Alkan, N., Altmuller, J., Alvarado-Balderrama, L., Bauser, C. A., Becker, C., Birren, B. W., Chen, Z. H., Choi, J., Crouch, J. A., Duvick, J. P., Farman, M. A., Gan, P., Heiman, D., Henrissat, B., Howard, R. J., Kabbage, M., Koch, C., Kracher, B., Kubo, Y., Law, A. D., Lebrun, M. H., Lee, Y. H., Miyara, I., Moore, N., Neumann, U., Nordstrom, K., Panaccione, D. G., Panstruga, R., Place, M., Proctor, R. H., Prusky, D., Rech,

G., Reinhardt, R., Rollins, J. A., Rounsley, S., Schardl, C. L., Schwartz, D. C., Shenoy, N., Shirasu, K., Sikhakolli, U. R., Stuber, K., Sukno, S. A., Sweigard, J. A., Takano, Y., Takahara, H., Trail, F., van der Does, H. C., Voll, L. M., Will, I., Young, S., Zeng, Q. D., Zhang, J. Z., Zhou, S. G., Dickman, M. B., Schulze-Lefert, P., van Themaat, E. V. L., Ma, L. J., and Vaillancourt, L. J. 2012. Lifestyle transitions in plant pathogenic *Colletotrichum* fungi deciphered by genome and transcriptome analyses. Nat. Genet. 44:1060-1065.

Petersen, T. N., Brunak, S., von Heijne, G., and Nielsen, H. 2011. SignalP 4.0: discriminating signal peptides from transmembrane regions. Nat. Methods 8:785–786.

Pettolino, F. A., Walsh, C., Fincher, G. B., and Bacic, A. 2012. Determining the polysaccharide composition of plant cell walls. Nat. Protoc. 7:1590-1607.

Qi, T., Guo, J., Liu, P., He, F. X., Wan, C. P., Islam, M. A., Tyler, B. M., Kang, Z. S., and Guo, J. 2019a. Stripe rust effector *Pst*GSRE1 disrupts nuclear localization of ROS-promoting transcription factor TaLOL2 to defeat ROS-induced defense in wheat. Mol. Plant 12:1624–1638.

Qi, T., Guo, J., Peng, H., Liu, P., Kang, Z. S., and Guo, J. (2019b) Host-induced gene silencing: a powerful strategy to control diseases of wheat and barley. Inter. Mol. Sci. 20:206.

Roberts, A., Pimentel, H., Trapnell, C., and Pachter, L. 2011. Identification of novel transcripts in annotated genomes using RNA-Seq. Bioinformatics 27:2325–

2329.

Robinson, M. D., McCarthy, D. J., and Smyth, G. K. 2010. edgeR: a Bioconductor package for differential expression analysis of digital gene expression data. Bioinformatics 26:139-140.

Ruske, E. and Dörfelt, H. 2010. Studies on the life history of the Mahonia rust (*Cumminsiella mirabilissima*). Boletus 32:78–88.

Rutter, W. B., Salcedo, A., Akhunova, A., He, F., Wang, S. C., Liang, H. Q., Bowden, R. L., and Akhunov, E. 2017. Divergent and convergent modes of interaction between wheat and *Puccinia graminis* f. sp *tritici* isolates revealed by the comparative gene co-expression network and genome analyses. BMC Genomics 18:291.

Schafer, W. 1993. The role of cutinase in fungal pathogenicity. Trends Microbio. 1:69–71.

Schwessinger, B., Sperschneider, J., Cuddy, W. S., Garnica, D. P., Miller, M. E., Taylor, J. M., Dodds, P. N., Figueroa, M., Park, R. F., and Rathjen, J. P. 2018. A Near-complete haplotype-phased genome of the dikaryotic wheat stripe rust fungus *Puccinia striiformis* f. sp *tritici* reveals high interhaplotype diversity. Mbio 9:e02275-17.

Sperschneider, J., Dodds, P. N., Gardiner, D. M., Singh, K. B., and Taylor, J. M. 2018. Improved prediction of fungal effector proteins from secretomes with EffectorP 2.0. Mol. Plant Pathol. 19:2094-2110.

Struck, C. 2015. Amino acid uptake in rust fungi. Front. Plant Sci. 6:40.

Trapnell, C., Roberts, A., Goff, L., Pertea, G., Kim, D., Kelley, D.R., Pimentel, H., Salzberg, S. L., Rinn, J. L., and Pachter, L. 2012. Differential gene and transcript expression analysis of RNA-seq experiments with TopHat and Cufflinks. Nat. Protoc. 7:562–578.

Upadhyaya, N. M., Garnica, D. P., Karaoglu, H., Sperschneider, J., Nemri, A., Xu, B., Mago, R., Cuomo, C. A., Rathjen, J. P., Park, R. F., Ellis, J. G., and Dodds, P. N. 2015. Comparative genomics of Australian isolates of the wheat stem rust pathogen *Puccinia graminis* f. sp *tritici* reveals extensive polymorphism in candidate effector genes. Front. Plant Sci. 5:759.

Updegraff, D. M. 1969. Semimicro determination of cellulose in biological materials. Anal. Biochem. 32:420-424.

Wang, B., Sun, Y. F., Song, N., Zhao, M. X., Liu, R., Feng, H., Wang, X. J., and Kang, Z.S. 2017. *Puccinia striiformis* f. sp *tritici* microRNA-like RNA 1 (*Pst*-milR1), an important pathogenicity factor of *Pst*, impairs wheat resistance to *Pst* by suppressing the wheat pathogenesis-related 2 gene. New Phytol. 215:338–350.

Wang, M. N. and Chen, X. M. 2013 First report of Oregon grape (*Mahonia aquifolium*) as an alternate host for the wheat stripe rust pathogen (*Puccinia striiformis* f. sp *tritici*) under artificial inoculation. Plant Dis. 97:839–839.

Xu, Q., Tang, C. L., Wang, X. D., Sun, S. T., Zhao, J. R., Kang, Z. S., and Wang, X. J. 2019. An effector protein of the wheat stripe rust fungus targets chloroplasts

and suppresses chloroplast function. Nat. Commun. 10:5571.

Yadav, I. S., Sharma, A., Kaur, S., Nahar, N., Bhardwaj, S. C., Sharma, T. R., and Chhuneja, P. 2016. Comparative temporal transcriptome profiling of wheat near isogenic line carrying *Lr57* under compatible and incompatible interactions. Front. Plant Sci. **7**:1943.

Yang, Q., Huai, B. Y., Lu, Y. X., Cai, K. Y., Guo, J., Zhu, X. G., Kang Z. S., and Guo, J. 2020. A stripe rust effector *Pst*18363 targets and stabilises TaNUDX23 that promotes stripe rust disease. New Phytol. 225:880–895.

Yu, G. C., Wang, L. G., Han, Y. Y. and He, Q. Y. 2012. clusterProfiler: an R package for comparing biological themes among gene clusters. Omics 16:284-287.

Zhang, H., Yohe, T., Huang, L., Entwistle, S., Wu, P. Z., Yang, Z. L., Busk, P. K., Xu, Y., and Yin, Y. B. 2018. dbCAN2: a meta server for automated carbohydrate-active enzyme annotation. Nucleic Acids Res. 46:W95–W101.

Zhao, J., Wang, L., Wang, Z. Y., Chen, X. M., Zhang, H. C., Yao, J. N., Zhan, G. M., Chen, W., Huang, L. L., and Kang, Z. S. 2013. Identification of eighteen *Berberis* species as alternate hosts of *Puccinia striiformis* f. sp *tritici* and virulence variation in the pathogen isolates from natural infection of barberry plants in China. Phytopathology 103:927–934.

Zhao, J., Wang, M. N., Chen, X. M., and Kang, Z. S. 2016. Role of alternate hosts in epidemiology and pathogen variation of cereal rusts. Annu Rev. Phytopathol. 54:207–228.

Zhao, M. X., Wang, J. F., Ji, S., Chen, Z. J., Xu, J. H., Tang, C. L., Chen, S. T., Kang, Z. S., and Wang, X. J. 2018. Candidate effector *Pst*_8713 impairs the plant immunity and contributes to virulence of *Puccinia striiformis* f. sp *tritici*. Front. Plant Sci. 9:1294.

Zhao, Z. T., Liu, H. Q., Wang, C. F., and Xu, J. R. 2013. Comparative analysis of fungal genomes reveals different plant cell wall degrading capacity in fungi. BMC Genomics 14:274.

Zheng, W. M., Huang, L. L., Huang, J. Q., Wang, X. J., Chen, X. M., Zhao, J., Guo, J., Zhuang, H., Qiu, C. Z., Liu, J., Liu, H. Q., Huang, X. L., Pei, G. L., Zhan, G. M., Tang, C. L., Cheng, Y. L., Liu, M., Zhang, J. S., Zhao, Z. T., Zhang, S. J., Han, Q. M., Han, D. J., Zhang, H. C., Zhao, J., Gao, X. N., Wang, J. F., Ni, P. X., Dong, W., Yang, L. F., Yang, H. M., Xu, J. R., Zhang, G. Y., and Kang, Z. S. 2013. High genome heterozygosity and endemic genetic recombination in the wheat stripe rust fungus. Nat. Commun. 4:2673.

Table 1. RNA-based sequence alignments against *Pst* CYR32 reference genome for normalized samples

Sample	Barberry infected by CYR32	Barberry infected by V26	Wheat infected by CYR32	Wheat infected by V26
Total reads	47893032	49554386	48957451	32164691
Total mapped	6250446(13.05%)	4856748(9.80%)	7081825(14.47%)	6365045(19.79%)
Total unmapped	41642586(86.95%)	44697638(90.20%)	41875626(85.53%)	25799646(80.21%)
Unique match	782080(1.63%)	398277(0.80%)	360634(0.74%)	150279(0.47%)
Mutliple match	5468366(11.42%)	4458471(9.00%)	6721191(13.73%)	6214766(19.32%)
Perfect match	5621223(11.74%)	4515399(9.11%)	6584063(13.45%)	5745820(17.86%)
<=5bp mismatch	591367(1.23%)	316156(0.64%)	485213(0.99%)	501987(1.56%)
Unique matched gene	17180	14032	11285	10554

Table 2. Number and proportion of orthologs identified from nine basidiomycetes for wheat-specifically expressed genes (WEGs) and barberry-specifically expressed genes (BEGs)

Species	WEGs (142)		BEGS (2677)	
	No. of Hits	Proportion (%)	No. of Hits	Proportion (%)
U. maydis	30	21.13	1074	40.12
M. osmundae	30	21.13	1186	44.30
N. fluitans	38	26.76	1231	45.98
M. larici-populina	55	38.73	1535	57.34
C. quercuum f. sp. *fusiforme*	59	41.55	1554	58.05
U. viciae fabae	67	47.18	1679	62.72
P. triticina	89	62.68	1991	74.37
P. graminis f. sp. *tritici*	91	64.08	2168	80.99
P. striiformis f. sp. *tritici* (*PST*-78)	118	83.10	2400	89.65

Fig. 1. Infection processes of *Puccinia striiformis* f. sp. *tritici* (*Pst*) basidiospores and urediniospores on barberry and wheat.

A, Microscopic observation of development processes of *Puccinia striiformis* f. sp. *tritici* (*Pst*) basidiospores and urediniospores on barberry and wheat. **B,** Penetration frequencies of *Pst* basidiospores and urediniospores on barberry and wheat during the early stage of infection. Penetration frequencies for *Pst* urediniospores on wheat leaves (blue) represent the percentage of germinated spores penetrating the mesophyll cells and forming haustoria. Penetration frequencies for *Pst* basidiospores on barberry leaves (red) represent the percentage of germinated spores penetrating into epidermal cells and forming ovate intra-epidermal vesicle. B: Basidiospore; OIV: ovate intra-epidermal vesicle; SH: secondary hyphae; H: haustorium; SSV: sub-stoma vesicle; HMC: haustorial mother cell; Bars, 10 μm. Each data point represents the mean ± SD of 3 replicates (leaves infected by *Pst* isolate CYR32).

Fig. 2. Identifying *Puccinia striiformis* f. sp. *tritici* genes specifically expressed in wheat or barberry.

A, Venn diagram depicting numbers of *Puccinia striiformis* f. sp. *tritici* (*Pst*) genes detected from normalized samples. W32 and B32 represent wheat and barberry leaves infected by isolate CYR32; W26 and B26 represent wheat and barberry leaves infected by isolate V26. **B,** The proportion of candidate secreted effector protein (CSEP) genes, hypothetical genes and functional annotated genes in wheat-specifically expressed genes (WEGs), barberry-specifically expressed genes (BEGs) and wheat-barberry expressed genes (WBEGs).

Fig. 3. *Puccinia striiformis* f. sp. *tritici* genes differentially expressed in wheat or barberry.

Scatter plot representing the relative gene expression levels of 1968 *Puccinia striiformis* f. sp. *tritici* (*Pst*) differentially expressed genes (DEGs) in wheat and barberry. *Pst* gene expression levels in barberry at 3 dpi (B_3dpi) vs in wheat at 1 dpi (W_1dpi) were plotted on x axis, and gene expression levels in barberry at 4 dpi (B_4dpi) vs in wheat at 2 dpi (W_2dpi) were plotted on y axis. Blue and red dots represents DEGs abundant in barberry and wheat, respectively. The dot color from light to deep indicates the adjust *P* value from big to small.

Fig. 4. Gene Ontology (GO) enrichment analysis of *Puccinia striiformis* f. sp. *tritici* differentially expressed genes between wheat and barberry.

Enrichment analysis of GO terms for *Puccinia striiformis* f. sp. *tritici* (*Pst*) differentially expressed genes (DEGs) abundant in wheat (A) and abundant in barberry (B) (p <0.05 with FDR correction). The R package of clusterProfiler were used for enrichment analysis (Yu et al. 2012).

Fig. 5. Heatmaps of gene expression showing *Puccinia striiformis* f. sp. *tritici* CSEP genes differentially expressed in wheat and barberry.

Hierarchical clustering of the expression levels (TPM values after the logarithm) of *Puccinia striiformis* f. sp. *tritici* (*Pst*) candidate secreted effector protein (CSEP) genes differentially expressed in wheat and barberry showing two distinct clades: clade I represent effector genes with higher expression levels in wheat at 1 or 2 dpi compared to that in barberry at 3 or 4 dpi; clade II contains most DEGs abundant in barberry. DEGs abundant in wheat which were identified as WEEs (wheat-specifically expressed effector genes) and WBEEs (wheat-barberry-commonly expressed effector genes) were in green and purple, while the others were in dark blue. DEGs abundant in barberry are in black.

Fig. 6. Inhibition of BAX-induced cell death by *Puccinia striiformis* f. sp. *tritici* (*Pst*) barberry-specifically expressed effector genes in tobacco.

Nicotiana benthamiana leaves were infiltrated with buffer ($MgCl_2$), *Agrobacterium tumefaciens* cells containing a vector carrying *Pst* candidate effector genes and a negative control gene (eGFP); 24 h later, *A. tumefaciens* cells carrying BAX were infiltrated at the same position according to the schematic diagram (left panel). The phenotype were photographed at 5 days post infiltrating with BAX (right panel).

Fig. 7. Expression profiling of *Puccinia striiformis* f. sp. *tritici* secreted cell-wall degrading enzyme genes and contents of wheat and barberry cell wall components. **A,** Expression levels (TPM values after the logarithm) of *Puccinia striiformis* f. sp. *tritici* (*Pst*) cell-wall degrading enzyme genes at 1&2 dpi of wheat and 3&4 dpi of barberry. **B,** Concentration of cell wall components of wheat and barberry leaves. Asterisks represent *Pst* differentially expressed genes in wheat and barberry.

Supporting Information

Supplementary Fig. S1: Sequencing saturation curves showing deep RNA sequencing of *Puccinia striiformis* f. sp. *tritici* for normalized (A) and non-normalized (B) cDNA library from barberry and wheat leaf samples.

Supplementary Fig. S2: KEGG enrichment analysis of *Puccinia striiformis* f. sp. *tritici* differentially expressed genes between wheat and barberry.

Supplementary Fig. S3: Phylogenetic tree of *Puccinia striiformis* f. sp. *tritici* (*Pst*) hexose transporters and their expression patterns during the early stage of wheat and barberry infection.

Supplementary Fig. S4: Expression patterns of *Puccinia striiformis* f. sp. *tritici* (*Pst*) amino acid transporters during the early stage of wheat and barberry infection.

Supplementary Table S1: RNA sequence alignments against *Puccinia striiformis* f. sp. *tritici* CYR32 reference genome for non-normalized samples.

Supplementary Table S2: List of 2712 new *Puccinia striiformis* f. sp. *tritici* genes identified in this study.

Supplementary Table S3: Gene expression levels of *Puccinia striiformis* f. sp. *tritici* in normalized wheat and barberry leaf samples.

Supplementary Table S4: *Puccinia striiformis* f. sp. *tritici* differentially expressed genes (DEGs) in wheat and barberry during the early stages of infection.

Supplementary Table S5: GO enrichment analysis of *Puccinia striiformis* f. sp. *tritici* DEGs abundant in barberry or wheat.

Supplementary Table S6: KEGG enrichment analysis of *Puccinia striiformis* f. sp. *tritici* DEGs abundant in barberry or wheat.

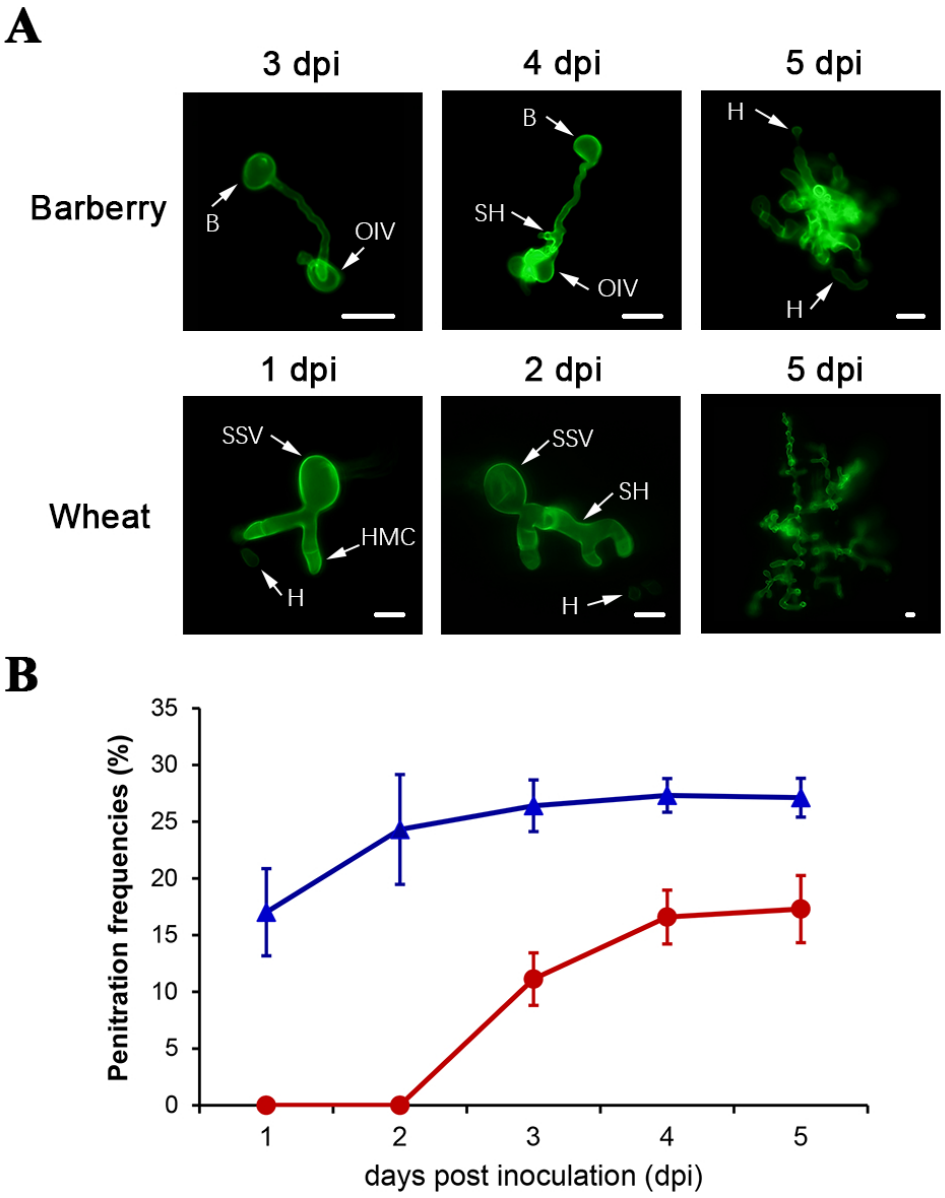

Fig. 1. Infection processes of Puccinia striiformis f. sp. tritici (Pst) basidiospores and urediniospores on barberry and wheat.

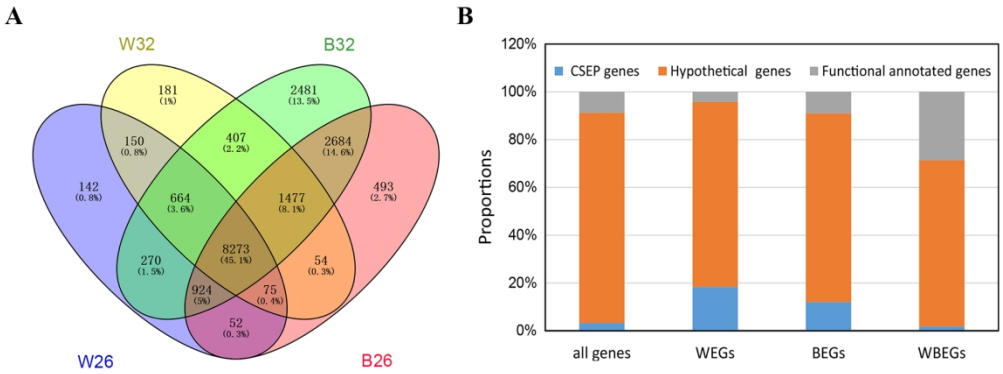

Fig. 2. Identifying Puccinia striiformis f. sp. tritici genes specifically expressed in wheat or barberry.

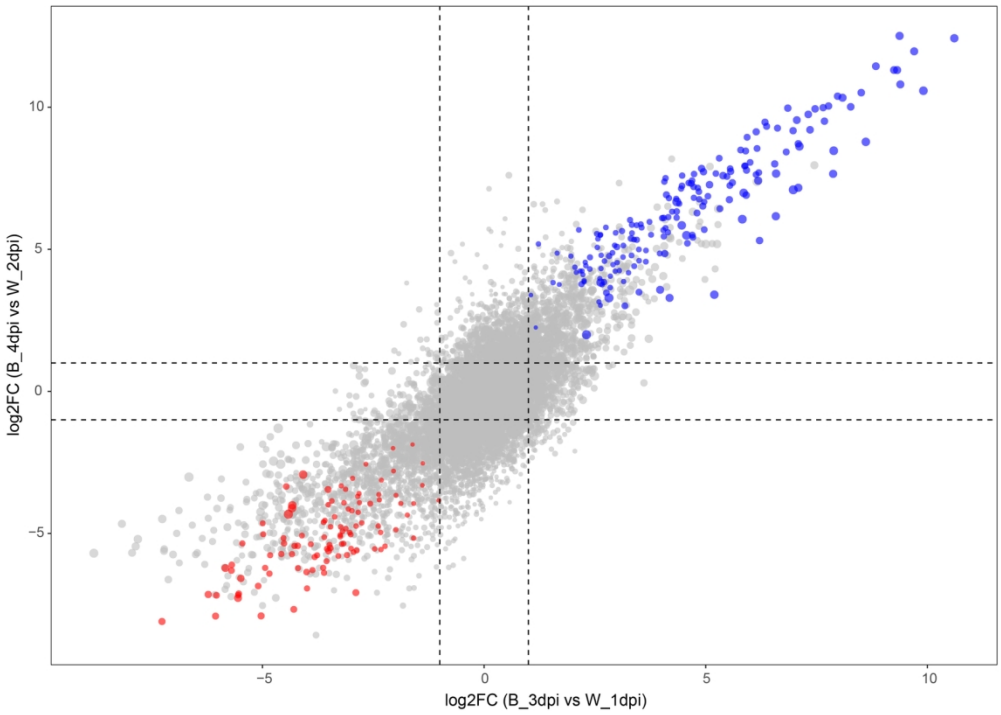

Fig. 3. Puccinia striiformis f. sp. tritici genes differentially expressed in wheat or barberry.

74x53mm (600 x 600 DPI)

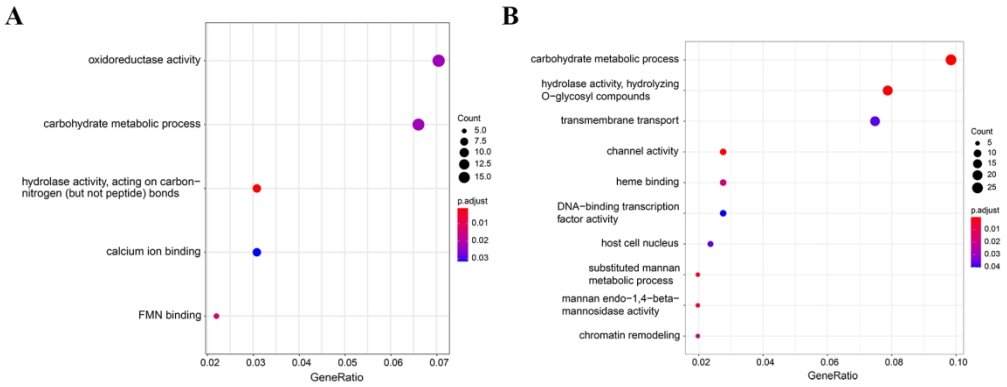

Fig. 4. Gene Ontology (GO) enrichment analysis of Puccinia striiformis f. sp. tritici differentially expressed genes between wheat and barberry.

158x60mm (300 x 300 DPI)

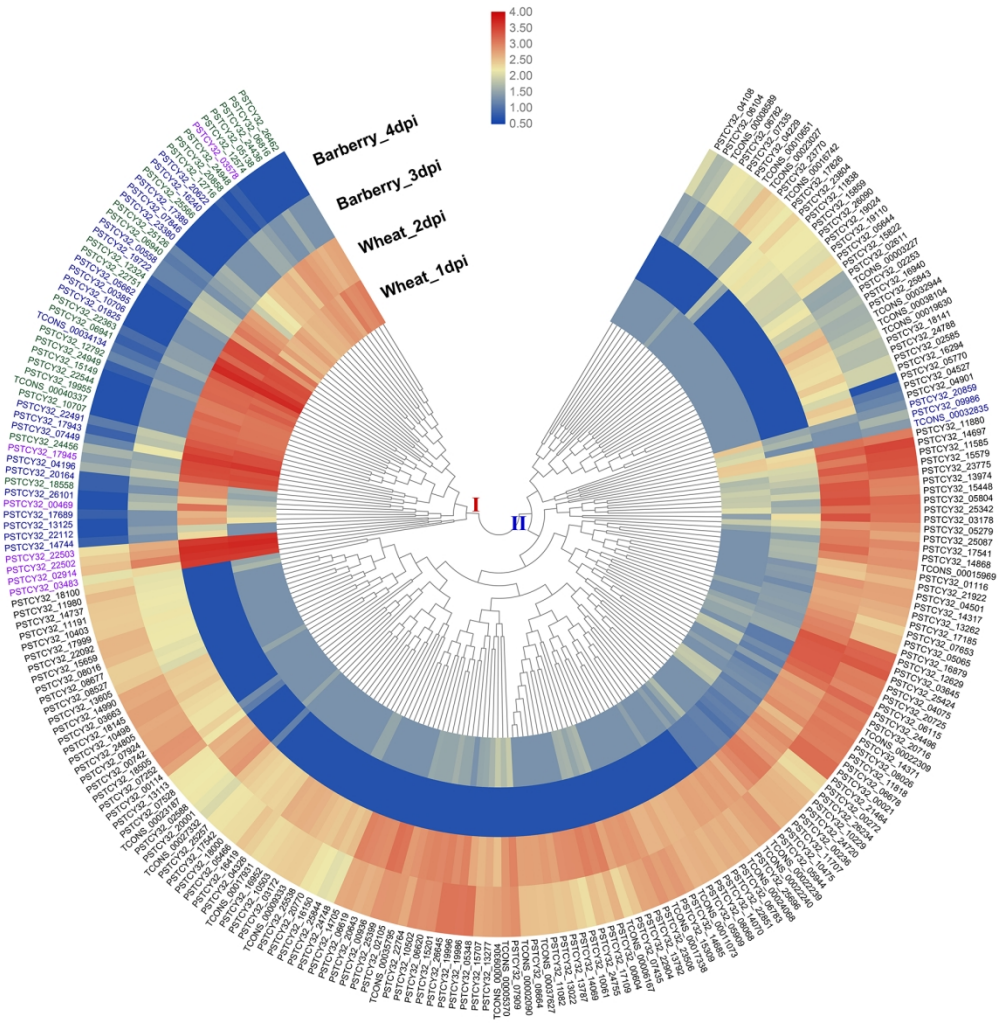

Fig. 5. Heatmaps of gene expression showing Puccinia striiformis f. sp. tritici CSEP genes differentially expressed in wheat and barberry.

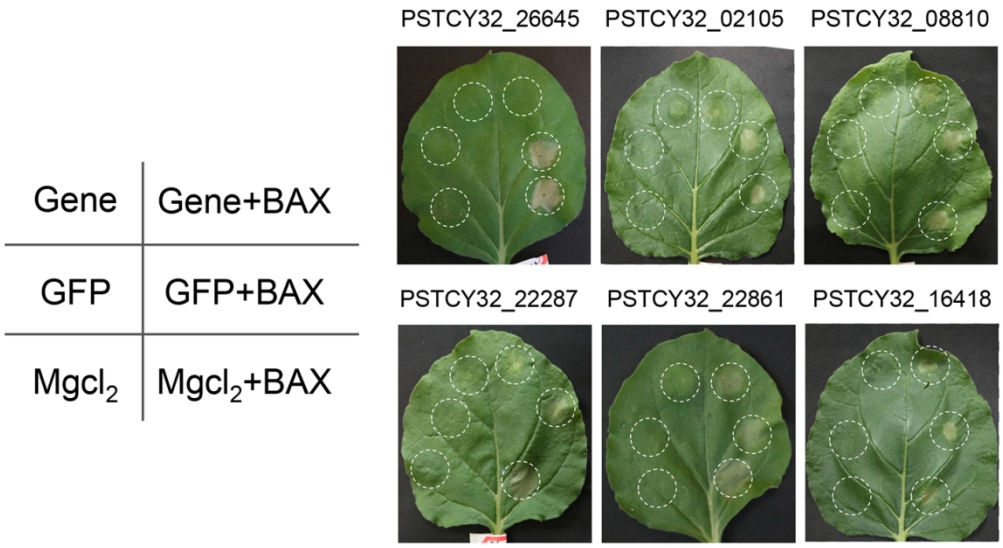

Fig. 6. Inhibition of BAX-induced cell death by Puccinia striiformis f. sp. tritici (Pst) barberry-specifically expressed effector genes in tobacco.

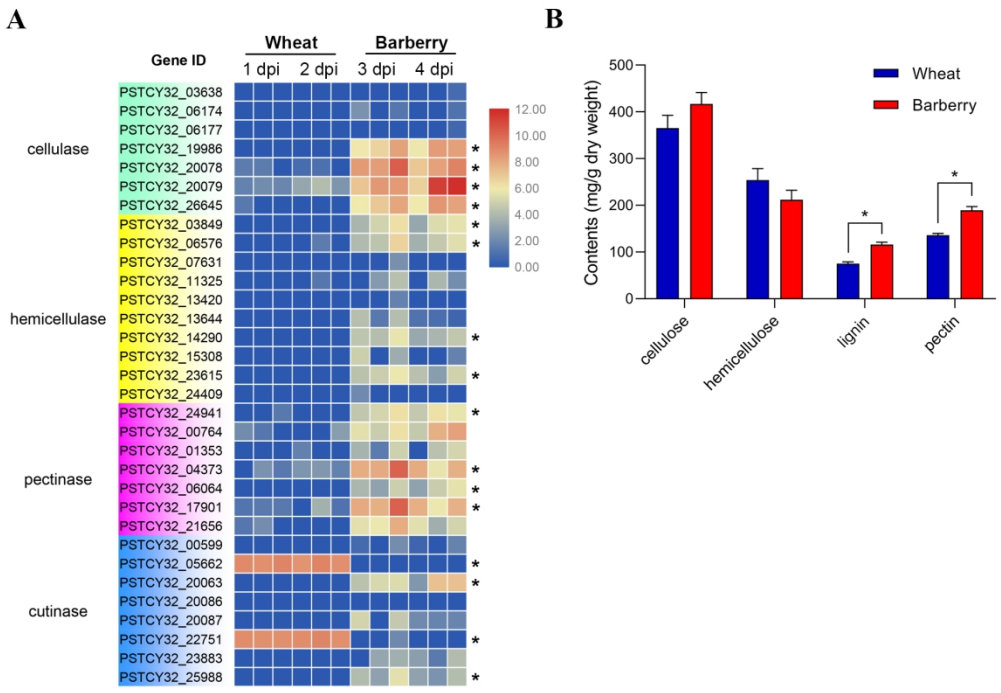

Fig. 7. Expression profiling of Puccinia striiformis f. sp. tritici secreted cell-wall degrading enzyme genes and contents of wheat and barberry cell wall components.

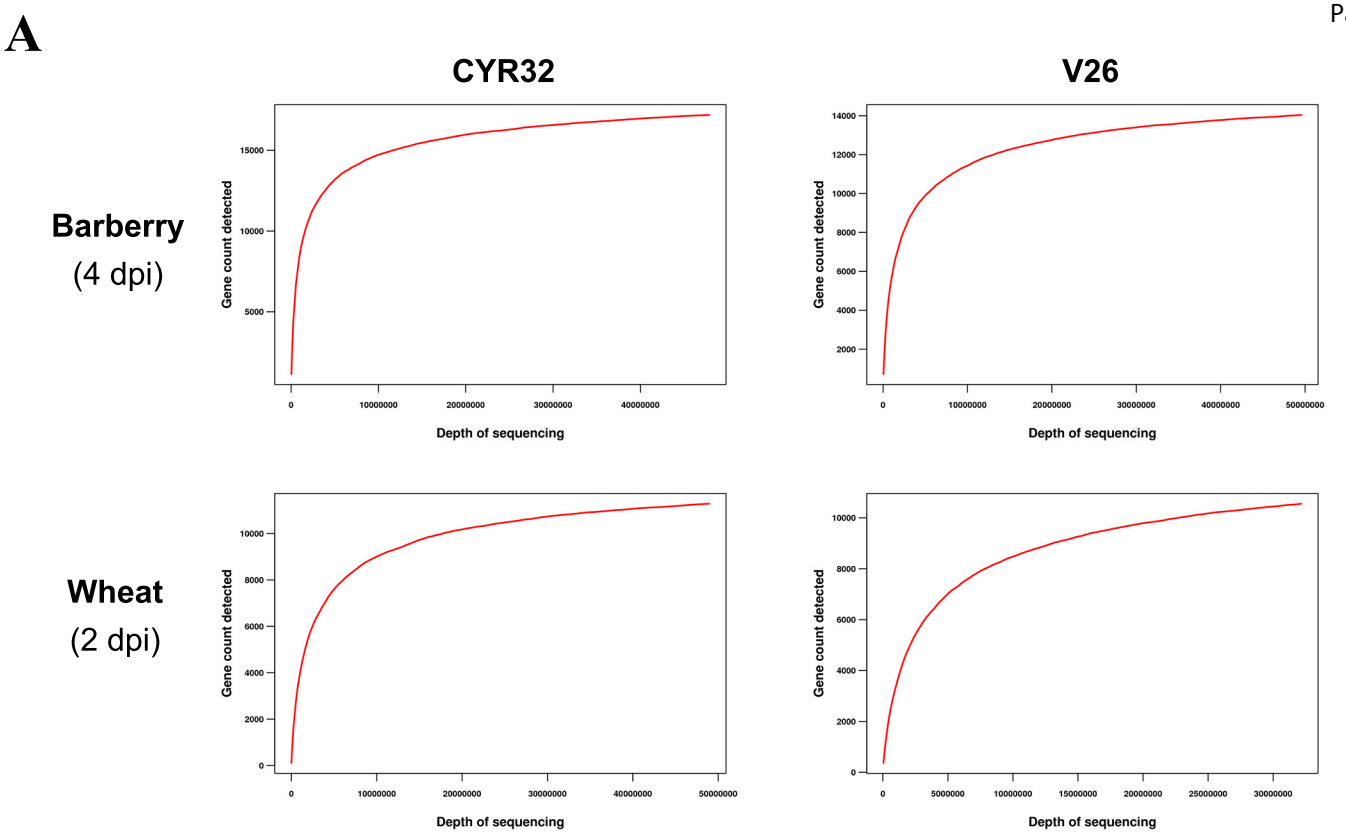

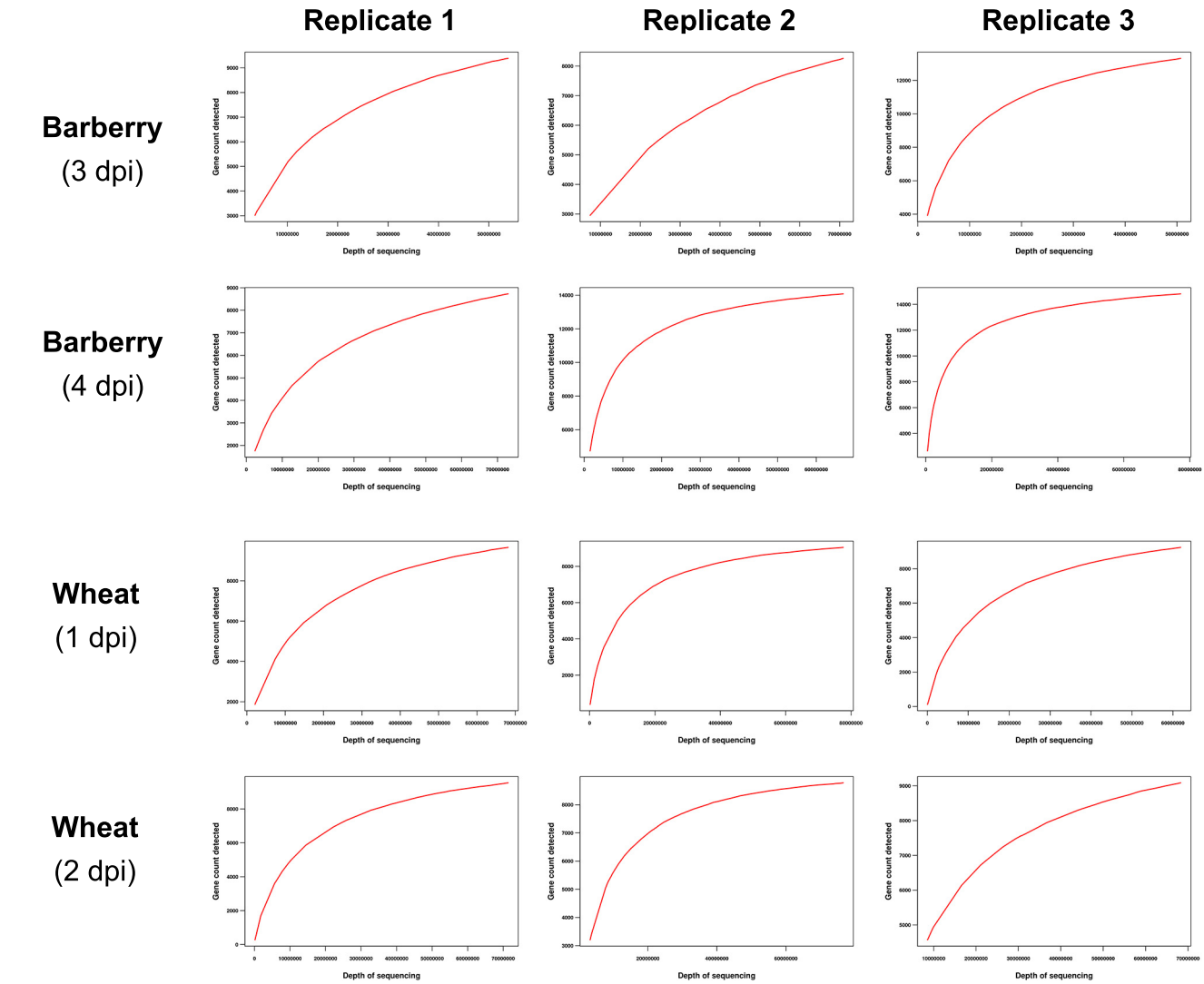

Supplementary Figure 1: Sequencing saturation curves showing deep RNA sequencing of *Puccinia striiformis* f. sp. *tritici* (*Pst*) during infection of barberry and wheat leaves.

A, normalized cDNA libraries from leaf samples infected by *Pst* isolates CYR32 and V26. **B,** non-normalized cDNA libraries from leaf samples infected by isolate CYR32.

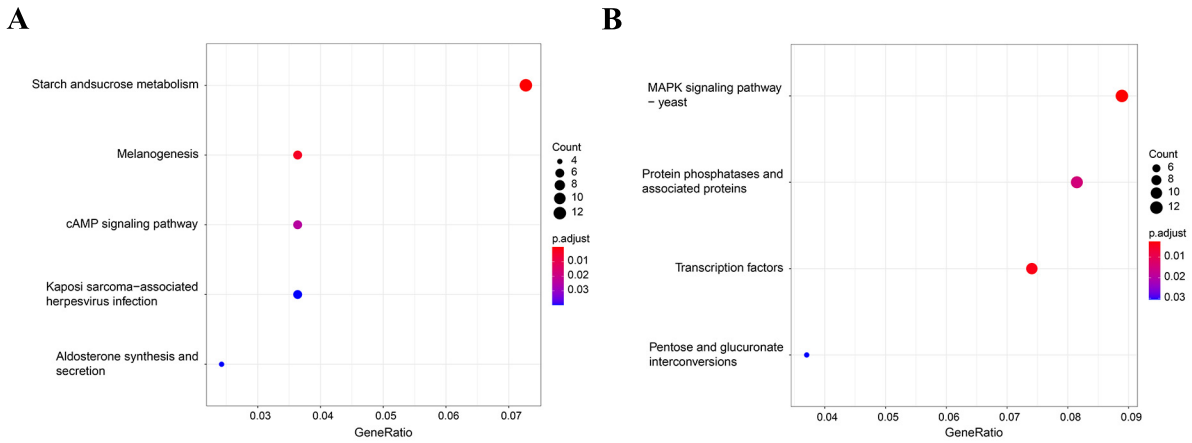

Supplementary Figure 2: KEGG enrichment analysis of *Puccinia striiformis* f. sp. *tritici* differentially expressed genes between wheat and barberry.

Enrichment analysis of KEGG pathways for *Puccinia striiformis* f. sp. *tritici* (*Pst*) differentially expressed genes (DEGs) abundant in wheat (A) and abundant in barberry (B) ($p < 0.05$ with FDR correction). The R package of clusterProfiler were used for enrichment analysis (Yu et al. 2012).

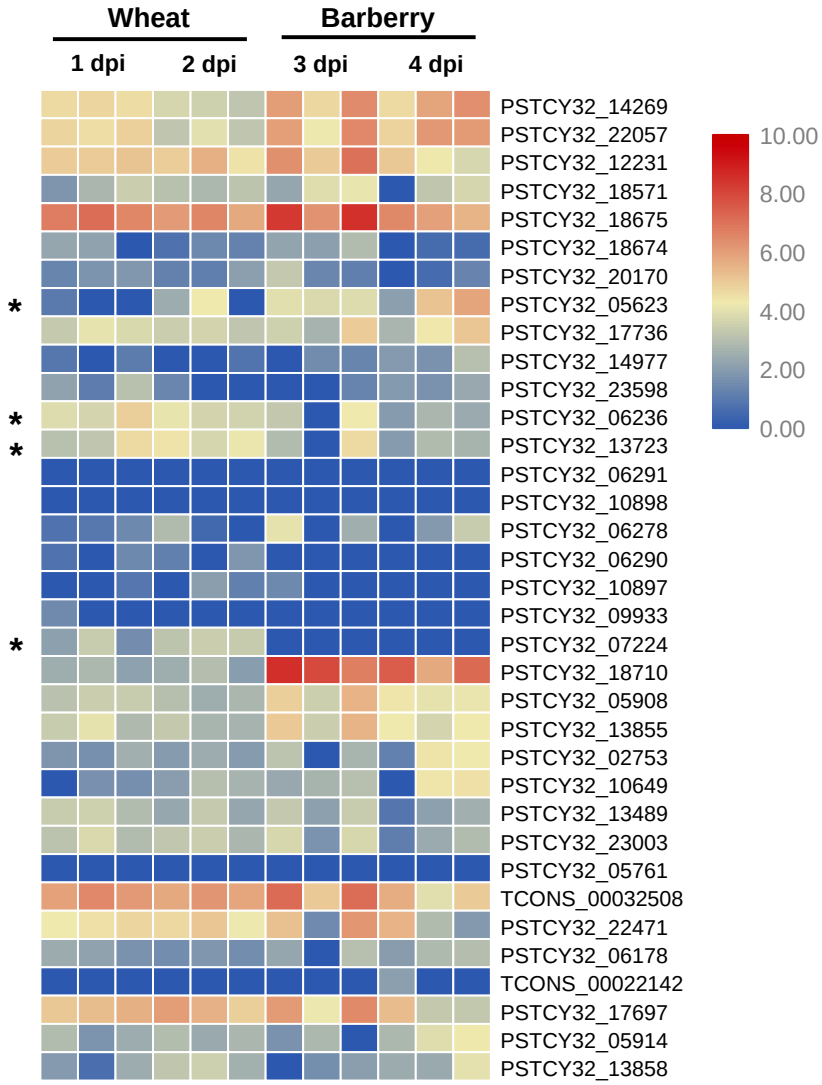

Supplementary Figure 3: Expression patterns of *Puccinia Striiformis* f. sp. *tritici* (*Pst*) hexose transporters during the early stage of wheat and barberry infection.

The $\log_2$(TPM+1) values of *Pst* hexose transporter genes in wheat (at 1 dpi and 2dpi) and barberry (at 3 dpi and 4 dpi) were shown. Asterisks represent Pst differentially expressed genes in wheat and barberry.

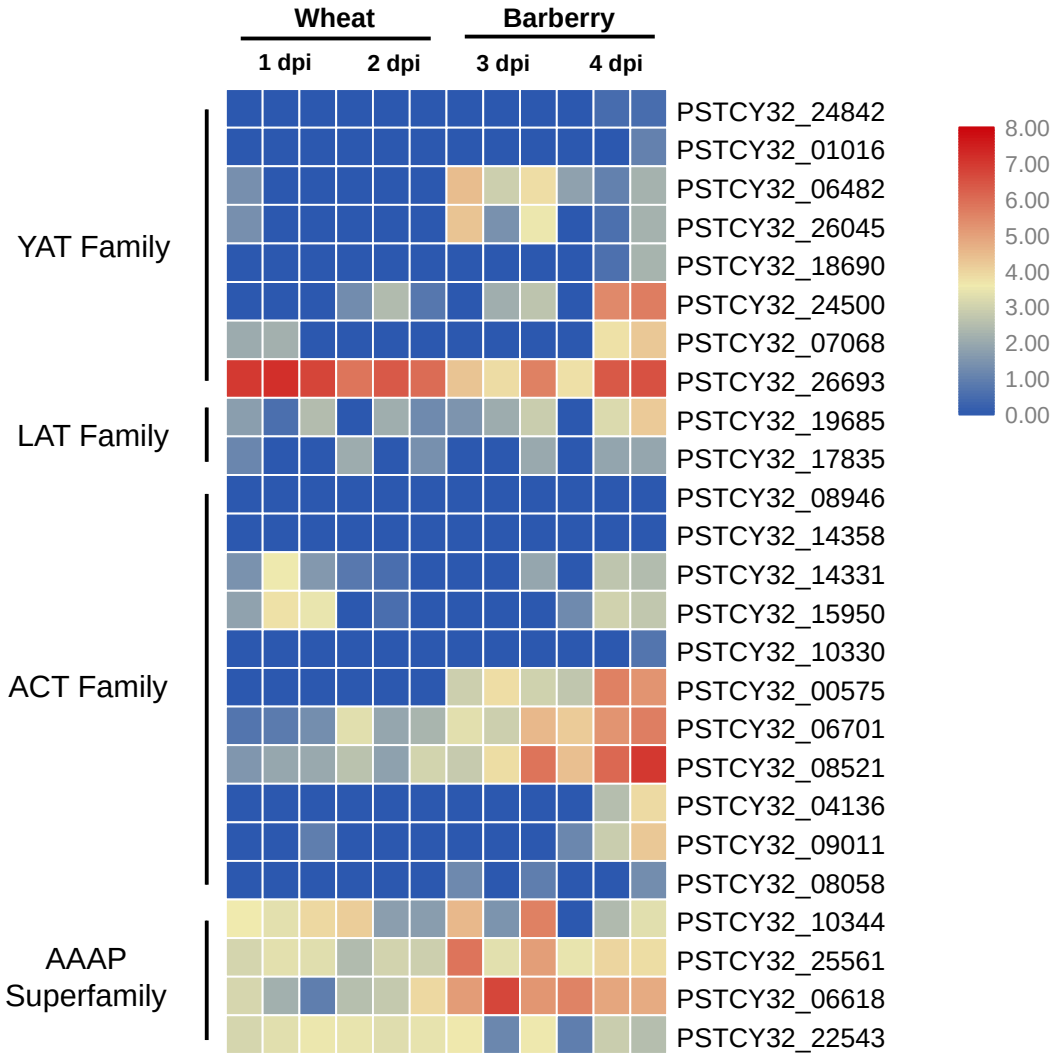

Supplementary Figure 4: Expression patterns of *Puccinia Striiformis* f. sp. *tritici* (*Pst*) amino acid transporters during the early stage of wheat and barberry infection.

The $\log_2$(TPM+1) values of *Pst* amino acid transporter genes in wheat (at 1 dpi and 2dpi) and barberry (at 3 dpi and 4 dpi) were shown. Asterisks represent Pst differentially expressed genes in wheat and barberry.